Geologische Rundschau **80/2** | 369–389 | Stuttgart 1991

Tectono-thermal evolution of a part of a Variscan magmatic arc: the Odenwald in the Mid-German Crystalline Rise

By A. P. WILLNER, H.-J. MASSONNE and A. KROHE, Bochum*)

With 4 figures and 6 tables

Zusammenfassung

Geothermobarometrische Untersuchungen an Plutoniten und mittel- bis hochgradigen Metamorphiten des Odenwaldes ermöglichen die Konstruktion von PT-Pfaden für vier Krustenabschnitte in einem Teil eines variszischen magmatischen Gürtels.

Zu Beginn der Entwicklung der thermischen Struktur des magmatischen Gürtels stellte sich ein Geotherm von 35–40°C/km nach einer Krustenstapelung ein, in die Gesteine mit Mitteldruckrelikten einbezogen wurden. Die PT-Bedingungen zum Höhepunkt der Metamorphose erreichten 4–5 kbar und 650°C. Nur Gesteine des nördlichen Odenwaldes belegen PT-Bedingungen, die auf einen höheren Geotherm zu dieser Zeit hinweisen. Frühe Hebung fand entlang von Schrägabschiebungen statt. Der zentrale Odenwald wurde bei gleichzeitiger Intrusion kalkalkaliner Magmen in ein Niveau entsprechend 3 kbar gehoben. Der nördliche Odenwald sank gleichzeitig ab, wie durch einen gegen den Uhrzeigersinn gerichteten PT-Pfad belegt wird. Im südlichen und östlichen Odenwald bewirkte danach schnelle Hebung einen weiteren Anstieg des Geotherms auf 60–80°C/km verbunden mit Dehnung und Intrusion granitoider Magmen.

Während Krustenverdickung auf eine frühe Phase im Devon beschränkt ist, entwickelt sich der magmatische Gürtel im Bereich des Odenwaldes im Unterkarbon innerhalb einer »pull apart«-ähnlichen Struktur.

Abstract

Geothermobarometric studies of plutonic and medium to high grade metamorphic rocks of the Odenwald (SW Germany) provide data for the construction of PT-paths of four different crustal sections within a part of a magmatic arc of the Mid-European Hercynian orogen.

The evolution of the thermal structure of the Odenwald is characterized by an early geotherm of 35–40°C/km after crustal stacking involving rocks with medium pressure relics. Peak PT-conditons reached 4–5 kbar and 650°C. Only rocks of the northernmost Odenwald show evidence for PT conditions related to a higher geotherm at this time. Early uplift occurred during normal oblique sinistral strike shear. The central Odenwald was uplifted into a level corresponding to 3 kbar during intrusion of calcalkaline magmas. The northernmost Odenwald subsided at the same time, as proved by an anticlockwise PT-path. Subsequently, in the southern and eastern Odenwald, rapid uplift caused a further increase of the geotherm to 60–80°C/km. This is concomitant with extension and granitoid intrusions.

Crustal thickening in the Odenwald is restricted to an early phase during the Devonian. The magmatic arc developed within a »pull-apart«-like structure during the Lower Carboniferous.

Résumé

Dans l'Odenwald (sud-ouest de l'Allemagne), l'étude géothermobarométrique de roches plutoni-

Author's adress: A. P. WILLNER, H.-J. MASSONNE, Institut für Mineralogie, Ruhr-Universität, Postfach 102 148, D-4630 Bochum, FR Germany and A. KROHE, Institut für Geologie, Ruhr-Universität, Postfach 102 148, D-4630 Bochum, FR Germany.

Manuscript received: 31. 5. 1990; accepted: 22. 3. 1991

ques et de roches métamorphiques de degré moyen à élevé fournit les données qui permettent la construction de trajets (P, T) relatifs à quatre sections crustales dans une partie d'un arc magmatique de l'orogène varisque d'Europe.

Le début de l'évolution de la structure thermique de l'Odenwald a été marqué par un gradient géothermique de 35–40°C/Km, en suite à un empilement crustal impliquant des roches qui contiennent des reliques de pression moyenne. Les conditions (P, T) du métamorphisme maximal furent de 4–5 Kbar et 650°C. Seules les roches de l'Odenwald septentrional témoignent d'un gradient plus élevé à cette époque. Un soulèvement hâtif s'est produit le long de zones de cisaillement sénestres. Concomitamment à l'intrusion de magmas calcoalcalins, l'Odenwald central a été le siège d'un soulèvement jusqu'à un niveau correspondant à 3 Kbar. En même temps, l'Odenwald septentrional s'affaissait, comme en témoigne uu trajet (P, T) anti-horlogique. Par la suite, dans l'Odenwald méridional et oriental, une montée rapide associée à un processus d'extension et à l'intrusion de magmas granitoïdes a amené le gradient géothermique à des valeurs de 60 à 80° /Km.

L'épaississement crustal est cantonné à une phase précoce d'âge dévonien, tandis que l'arc magmatique s'est développé dans une structure »pull-apart« au cours du Carbonifère inférieur.

Краткое содержание

По результатам геотермобарометрических исследований изверженных пород и метаморфических пород средних и высоких ступеней из Оденвальда получены *PT*-тренды для четырех разрезов земной коры на участке герцинского магматического пояса.

Начальная стадия развития термической структуры Оденвальда, которая последовала за накоплением корового разреза, содержащего реликты метаморфических пород умеренного давления, характеризуется геотермой 35–40°C/км. *PT*-условия пика метаморфизма оцениваются как 650°Си 4–5 кбар, и лишь для самой северной части Оденвальда получены *PT*-оценки, соответствующие более высокой геотерме того времени. Раннее поднятие происходило вдоль косых сбросов. Центральная часть Оденвальда испытала поднятие до уровня, соответствующего давлению 3 кбар, в связи с интрузией известково-щелочных магм. Одновременно происходило опускание северной части, которое характеризуется *PT*-трендом, направленным против часовой стрелки. За этими событиями последовало быстрое поднятие геотермы южной и восточной частей Оденвальда до 60–80°C/км, связанное с растяжением и гранитоидными интрузиями.

В то время как процесс утолщения коры ограничен ранней стадией, относящейся к девону, развитие магматического пояса Оденвальда связано с образованием структур типа »pull-apart« в нижнем карбоне.

1. Introduction

The Odenwald is the largest exposure of the Mid-German Crystalline Rise (Fig. 1), a zone of the Mid-European Variszides that is characterized by intermediate- to low-pressure, amphibolite-facies metamorphism (OKRUSCH, 1983; OKRUSCH, et al. 1975) and a synorogenic suite of multiple, calc alkaline intrusions (NICKEL & MAGGETTI, 1974; MAGGETTI, 1975). It is therefore interpreted as a deeply eroded magmatic arc (LORENZ & NICHOLLS, 1984; LIEW & HOFMANN, 1988; HENES-KLAIBER et al., 1989). To the north, the Mid-German Crystalline Rise is bounded by the Northern Phyllite Zone, a belt of very low to low grade metamorphic rocks, including some with high-pressure imprint (MASSONNE & SCHREYER, 1983). This zone is followed to the north by the Rhenohercynian Zone, which represents a foreland thrust belt mainly of Upper Paleozoic sediments (WEBER & BEHR, 1983). Relics of an oceanic crust and fore-arc sediments are found in the Giessen-Harz Nappe Zone emplaced on top of the Rhenohercynian (FRANKE, 1989). The Saxothuringian Zone sensu strictu lies south of the Mid-German Crystalline Rise. It includes large areas of parautochthonous Paleozoic sediments (FRANKE, 1989). The Northern Phyllite Zone and the Mid-German Crystalline Rise are interpreted as a paired metamorphic belt with a southward directed subduction zone along a suture south of the Rhenohercynian (LORENZ & NICHOLLS, 1984; NEUGEBAUER, 1988).

The scope of the present paper is to obtain a better understanding of the magmatic history and the crustal dynamics of the Mid-German Crystalline Rise as a Variscan magmatic arc. Geothermobarometric data for different crustal sections of the Odenwald were therefore derived and correlated with three distinct successive deformation events (KROHE, 1991a, b) of different regimes (compres-

sive, transtensional, extensional). The results show, how these deformational events disturbed the thermal structure of the crust. Intrusion ages (KIRSCH et al., 1988) and K/Ar biotite and hornblende cooling ages (KREUZER & HARRE, 1975; RITTMANN, 1984; HESS & SCHMIDT, 1989; LIPPOLT, 1986) provide an approximate absolute time frame.

2. Geological setting of the Odenwald

The Odenwald was subdivided by KROHE (1991a) into four crustal sections of different evolution (Fig. 1). All units display a polyphase deformation history. Structures that developed before or near the thermal peak of metamorphism are arbitrarily termed D_1/D_2 (KROHE, 1991a). These structures may not reflect distinct tectonic events within a single unit and the units are also characterized by different early tectonic histories. Structures that developed after the thermal peak of metamorphism have been termed D_3 and D_4 (KROHE, 1991a, b). These deformations are localized in shear zones along which the different units were emplaced. D_3 describes a tectonic episode of transtension occurring between 360 and 340 Ma (KROHE, 1991b). It is followed by a horizontal extension D_4. The minimum age for D_4 is 330 Ma according to HESS & SCHMIDT (1989) who have dated an undeformed lamprophyre in D_4-cataclasites.

Unit I is dominated by amphibolites and subordinate paragneisses showing a penetrative D_1/D_2-foliation. These rocks were intruded by gabbros, diorites and subordinate granodiorites and granites, all of which remained predominantly undeformed. K/Ar hornblende cooling ages for the gabbros of the Frankenstein pluton and the granodioritic intrusion east of Darmstadt yielded a mean of 363 Ma (KIRSCH et al. 1988) and 344 Ma, respectively (KREUZER & Harre, 1975).

In Unit II two major, relatively narrow zones of medium to high grade para- and orthogneisses with subordinate amphibolites are present. They were described by NICKEL (1985) as Neutsch Complex in the north and Heppenheimer Schieferzug in the south. These zones were affected by strong mylonitisation D2 (KROHE, 1991a). The central part of unit II was intruded by a voluminous calc alkaline suite, ranging from gabbros to granites with mean K/Ar hornblende cooling ages of 342 Ma (KREUZER & HARRE, 1975; RITTMANN, 1984). This zone was described by NICKEL & MAGGETTI (1974) as Neunkirchen Intrusive Complex. The entire calc alkaline suite was deformed together with the wall rocks by sinistral strike-slip movements (D_3 after KROHE, 1991a, b) with locally varying intensities. Many plutons intruded during D_3. This deformation is confined mainly to unit II.

Unit III is characterized by granodioritic and granitic plutons containing large blocks of partly migmatized wall rocks, both paragneisses and amphibolites. The intrusions postdate D_3. They were emplaced into an extensional regime (D_4 after KROHE, 1991a). Normal fault zones defining this deformational event are ubiquitous. They also define the border towards units IV (Otzberg Zone in NICKEL, 1985) and II (Fig. 1). The mean K/Ar hornblende cooling age of the intrusions is 335 Ma (KREUZER & HARRE, 1975).

Unit IV consists of paragneisses and granitic to granodioritic orthogneisses that underwent polyphase deformation (D_1/D_2). The orthogneisses are regarded as intrusions of Late Silurian age (LIPPOLT, 1986). A discordant U/Pb zircon age of 380 Ma is interpreted as an early metamorphic event by TODT (1979). The dominant transposition schistosity s_2 is deformed by a large-scale antiform with NNW-SSE strike (CHATTERJEE, 1960). KROHE (1991a) relates this antiform to D_4.

3. Geothermobarometric methods

Similar geothermobarometric methods were applied as extensively as possible in order to allow a better comparison between the PT-data of different units. An attempt was made to determine every PT-datum with at least two independent methods. These are described below:

Method 1: Multivariant mineral equilibria were calculated using the thermodynamic data set of BERMAN (1988). This method was applied only to garnet-bearing parageneses involving the endmembers muscovite, phlogopite, annite, anorthite, sillimanite, kyanite, clinochlore, tremolite, clinozoisite, pyrope, almandine and grossular. The corresponding activity models are based on the assumption of ideal mixing and are given Table 1. The thermodynamic data ΔH_f° and S° of annite were added to Berman's data set by fitting the experimental results of FERRY & SPEAR (1978) on the Fe-Mg-exchange between garnet and biotite using the activity models given in Table 1. The c_p-function of annite was estimated according to BERMAN & BROWN (1985). The a_p- and β_T-functions were assumed to be identical to those of phlogopite as given by BERMAN (1988). The molar volume of annite was taken from HOLLAND & POWELL (1990).

Method 2: Following to SPEAR & SELVERSTONE (1983), P and T were estimated from the molar proportion of both Fe-endmembers of garnet and biotite in contact with quartz, sillimanite and muscovite.

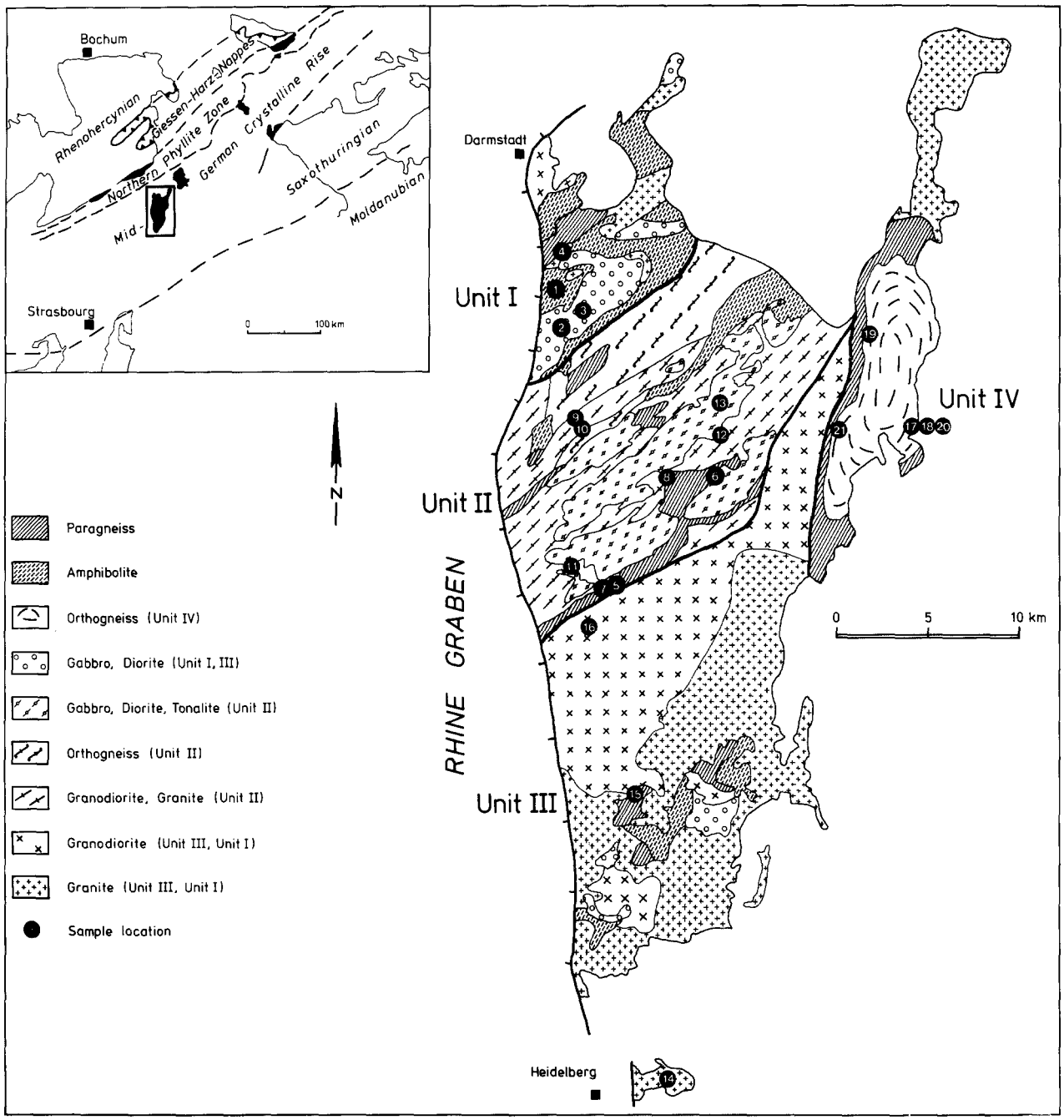

Fig. 1. Lithological map and regional setting of the Odenwald (insert map).

Method 3: The upper pressure stability limit of the assemblage cordierite + muscovite was recently redetermined experimentally by MASSONNE (1988) in the system K_2O-MgO-Al_2O_3-SiO_2-H_2O. Using in addition the corresponding reaction curve for the system K_2O-Al_2O_3-SiO_2-H_2O estimated from experimental data of HOLDAWAY & LEE (1977), a very sensitive geobarometer for the assemblage cordierite + muscovite + biotite + aluminosilicate + quartz results (MASSONNE, 1988). This barometer requires the knowledge of X_{Mg} of cordierite only.

Method 4: Metamorphic and plutonic rocks with the assemblage K-feldspar-quartz-biotite-muscovite were evaluated using phengite barometry as calibrated by MASSONNE & SCHREYER (1987). Thus, no correction for deviations of the chemical compositions of these minerals from the system K_2O-MgO-Al_2O_3-SiO_2-H_2O was applied. Because this type of barometry requires an independent temperature estimation, the following approaches were used:

a) In the case of most two-mica granites and anatectic gneisses, wet granite solidus temperatures given by JOHANNES (1984) were assumed in accordance with BURNHAM (1979) and ZEN (1989). The resulting pressure corresponds to an intrusion depth of the granitic magma (MASSONNE, 1984).

b) For several other two-mica granite samples, the Si-isopleths

Mineral phase	Component		Activity model
Amphibole:	Tremolite	$\square Ca_2Mg_5[Si_8O_{22}](OH)_2$	$X_{Si}^8 \cdot X_{Mg}^5 \cdot X_{Ca}^2 \cdot X_{\square} \cdot X_{OH}^2$
Biotite:	Annite	$KFe^{2+}{}_3[AlSi_3O_{10}](OH)_2$	$X_{Fe^{2+}}^3 \cdot X_K \cdot X_{OH}^2$
	Phlogopite	$KMg_3[AlSi_3O_{10}](OH)_2$	$X_{Mg}^3 \cdot X_K \cdot X_{OH}^2$
Chlorite:	Clinochlore	$Mg_5Al[AlSi_3O_{10}](OH)_8$	$X_{Si}^4 \cdot X_{Mg}^5 \cdot X_{OH}^8 \cdot 3.1605$
Epidote:	Clinozoisit	$Ca_2Al_3[Si_3O_{12}](OH)$	$X_{Al(M1)}$
Feldspar:	Anorthite	$CaAl_2Si_2O_8$	X_{Ca}
Garnet:	Almandine	$Fe^{2+}{}_3Al_2[SiO_4]_3$	$X_{Fe^{2+}}^3 \cdot X_{Al}^2$
	Grossular	$Ca_3Al_2[SiO_4]_3$	$X_{Ca}^3 \cdot X_{Al}^2$
	Pyrope	$Mg_3Al_2[SiO_4]_3$	$X_{Mg}^3 \cdot X_{Al}^2$
Muscovite:	Muscovite	$KAl_2[AlSi_3O_{10}](OH)_2$	$X_{Al^{VI}}^2 \cdot X_K \cdot X_{OH}^2$

X_{Si} = Si/(Si+Al^{IV})
X_{Al} = Al/(Al+Fe^{3+}), $X_{Al^{VI}}$(Muscovite) = $Al^{VI}/2$
$X_{Fe^{2+}}$ = Fe^{2+}/Fe^{2+}+Mg+Mn+Ca), $X_{Fe^{2+}}$(Annite) = $Fe^{2+}/3$,
X_{Mg} = Mg/(Fe^{2+}+Mg+Mn), X_{Mg}(Phlogopite) = $Fe^{2+}/3$,
X_{Mg}(Pyrope) = Mg/(Fe^{2+}+Mg+Mn+Ca)
X_{Ca}(Amph)= Ca/Ca+Na^{M4}), X_{Ca}(An) = Ca/(Ca+Na+K),
X_{Ca}(Gross) = Ca/(Ca+Fe^{2+}+Mg+Mn)
X_{Na}(Amph)= $Na^{M4}/(Ca+Na^{M4})$
X_K = K/(Ba+Ca+Na+K)
$X_{\square}$ = 1-(Ba+K+Na^A)
X_{OH} = OH/(OH+F)

Table 1. Activity models used for method 1 (see section 3).

intersect the muscovite + quartz breakdown curve (CHATTERJEE & JOHANNES, 1974). Here, muscovite formation is a subsolidus phenomenon, as demonstrated in part by symplectitic textures (see section 4). In this case the temperature of the muscovite + quartz breakdown was chosen. The same approach was used for HT retrograde muscovite growth from sillimanite in gneisses.

c) Somewhat lower temperatures (500°–600°C) than assumed for b) were taken for retrograde muscovite grown contemporaneously with recrystallising feldspar.

d) Temperatures between 400° and 500°C were suggested from concomitant retrograde mineral assemblages.

Method 5: Solidus temperature for an olivine gabbro were estimated with the aid of two-pyroxene-thermometers according to LINDSLEY (1983; method 5a in this paper) and WELLS (1977; method 5 b).

Method 6: The Tschermaks component of clinopyroxene coexisting with orthopyroxene-olivine-plagioclase was used to estimate the intrusion depth of an olivine gabbro according to HERZBERG (1978).

Method 7: Temperatures for the formation of amphibole-magnetite-ilmenite-symplectites occurring in a gabbro were estimated with the ilmenite-magnetite-thermometer (SPENCER & LINDSLEY, 1981; corrected by ANDERSEN & LINDSLEY, 1985).

Method 8: The hornblende-plagioclase geothermobarometer of PLYUSNINA (1982) was applied to rocks with hornblende, plagioclase and epidote.

Method 9: Temperatures obtained with method 8 were corroborated independently with the empirical plagioclase-hornblende thermometer of SPEAR (1980).

Method 10: Intrusion depths of granodiorites with the assemblage hornblende-K-feldspar-plagioclase-quartz-biotite-titanite-magnetite were estimated with the empirical igneous calcic-amphibole geobarometer of HAMMARSTROM & ZEN (1986), as improved by HOLLISTER et al. (1987). Only rims of hornblende and plagioclase were measured to ensure equilibrium during solidification.

Method 11: In the case of muscovite + quartz-breakdown to K-feldspar + sillimanite/andalusite, the intersection of the muscovite + quartz breakdown curve (CHATTERJEE & JOHANNES, 1974) with the andalusite-sillimanite transition of HOLDAWAY (1971) yields a further PT-datum.

4. Sample description

Twenty-three rock samples were used for geothermobarometry. The sample locations are given in Fig. 1 and Table 2. Brief petrographic descriptions and the geothermobarometric results extracted from these samples are listed in Table 3. Additional petrographic details are as follows:

Samples with garnet-bearing parageneses

Garnet-bearing parageneses occur in a variety of different rock types (samples 5, 8, 9, 17, 21):

In the paragneiss (*sample 5*) occurring in the southern part of unit II, the garnet-bearing paragenesis equilibrated after formation of an early schistosity which was also affected by the retrograde deformation D_3. The idiomorphic garnets contain only quartz as inclusions. They were slightly rotated by the D_3-deformation at high temperatures, as is shown by feldspar recrystallisation in pressure shadows. Biotite formed mimetically along the $s_{1/2}$-foliation, while muscovite grew later as xenomorphic grains partly replacing plagioclase, especially in that part of the rock which was strongly deformed by D_3. The muscovites are thought to be in equilibrium with garnet and biotite. Similar garnet-bearing parageneses were described by VON RAUMER (1973).

In the southern part of unit II garnet-cordierite-sillimanite-felses, called kinzigites (*sample 8*), are

Sample No.	*Locality*	*Coordinates*	
1	Road outcrop N` Frankenstein Castle	H 551775	R 347595
2	Quarry 1 km S` Frankenstein Castle	H 551675	R 347595
3	Quarry 500 m E` Niederbeerbach	H 551733	R 347740
4	Quarry E` Eberstadt	H 552057	R 347484
5	Silbergrubenkopf, W` Mittershausen	H 550215	R 347887
6	500 m E` Kolmbach	H 550778	R 348285
7	Silbergrubenkopf, W` Mittershausen	H 550330	R 347884
8	500 m E` Gadernheim	H 550862	R 348145
9	Helgengrund, 800 m E` Balkhausen	H 551078	R 347646
10	Felsberg, 1.3 km SSE` Balkhausen	H 551023	R 347594
11	500 m NW` Oberhambach	H 550392	R 347725
12	Rimdidim, SE` Steinau	H 551078	R 347646
13	Mühlberg quarry E` Billings	H 551305	R 348593
14	Railway bridge 1 km E` Heidelberg	H 547860	R 347657
15	Road outcrop 1.5 km SSE` Birkenau	H 548970	R 347995
16	Quarry Sonderbach	H 549765	R 347830
17	Quarry Wannberg	H 551862	R 349505
18	Quarry Wannberg	H 551862	R 349505
19	Road outcrop 1.5 km NE` Brensbach	H 551555	R 349252
20	Quarry Wannberg	H 551862	R 349505
21	500 m NE` Obergersprenz	H 551036	R 349155

Table 2. Sample locations. Coordinates refer to the German Gauß-Krüger-net.

found in lenses of several 100 m length. These lenses contain mainly graphitic quartzites and are intercalated between metapelites and deformed granitoids. The kinzigites have a polyphase history and an as yet unknown protolith. They were described by BÜSCH et al. (1980). These massive, coarse-grained rocks lack any preferred orientation. The garnets are usually several mm in diameter and hypidioblastic. Their cores show inclusions mainly of biotite, plagioclase and quartz, mostly in contact with each other, while the broad rims contain only a few inclusions of cordierite and plagioclase. This suggests two major stages of garnet growth. The edges of the garnets are partly rounded and coated with small rims of sillimanite and biotite, indicating that garnet was unstable during a final metamorphic stage. The matrix consists of slightly zoned plagioclase, cordierite with sillimanite inclusions, sillimanite, quartz and biotite; small grains of staurolite as inclusions in quartz and ilmenite are accessories. Muscovite, chlorite and andalusite are secondary phases.

Sample 10 is a HT-mylonite of granitic composition deformed by D_3 in the northern part of unit II. Idioblastic garnet as well as large, passively rotated muscovite are thought to be of magmatic origin. Biotite and smaller recrystallized muscovites show markedly preferred orientation parallel to the s_3-foliation. Quartz and both feldspars are entirely recrystallized. Symplectitic intergrowth with quartz can be observed in the small recrystallized muscovites, as well as at the edges of the larger magmatic muscovites. *Sample 9* is a similar rock, but without garnet.

Sample 14 within unit IV is a biotite-plagioclase-gneiss, which was named granodiorite gneiss by CHATTERJEE (1960). Garnets occur as inclusions in plagioclase and matrix biotite showing round or oval shaped grains of only 100–200 μm in diameter. The garnet inclusions in plagioclase are partly in contact with enclosed biotite. Kyanite also appears as inclusions in plagioclase. Biotites are roughly mimetical to an early $s_{1/2}$-foliation. The gneissose fabric is typical for long static annealing at high temperatures.

Samples with parageneses of both micas and K-feldspar

A variety of rocks of granitic composition and with the assemblage K-feldspar-quartz-biotite-muscovite, suitable for phengite barometry, are widespread in the entire Odenwald. Hence a good basis for comparison among the PT-data for the different units is given. However, these rocks comprise only a very small volume of the units studied.

Granite *samples 11 and 12* from the centre of unit II belong to a magmatic suite that intruded the high temperature mylonites samples 9 and 10 mentioned above. However, they also are slightly deformed by the same D_3-event. Feldspars are recrystallized in sample 11 and subjected to brittle deformation in sample 12. Symplectitic intergrowth with quartz is observed, where muscovites form aggregates of small, randomly orientated crystals.

A deformed, late granite vein (*sample 3*) in unit I shows recrystallisation of feldspars. Small muscovite-quartz symplectites occur, as well as retrograde muscovite in a veinlet intergrown with epidote, chlorite and calcite.

Sample 14 is a granitic vein from the southern part of unit III. Beside large magmatic muscovites also smaller retrograde muscovites appear intergrown with green biotites forming round pseudomorphs after either garnet or cordierite. As in sample 3 the retrograde muscovites are in mutual contact with biotite and K-feldspar.

In an anatectic mobilisate (*sample 18*) and a granite gneiss (*sample 19*) of unit IV muscovites have equilibrated at temperatures of the wet granite solidus, for concomitant anatectic phenomena are widespread in this zone.

Retrograde muscovites must have formed at somewhat lower temperatures in some gneisses (*samples 7a, b, 15 and 20*) in areas with widespread anatectic phenomena as in the southern part of unit II, in the wall rocks of unit III and in unit IV. Large xenoblastic muscovites grew across sillimanite that had formed earlier with K-feldspar from muscovite + quartz.

Samples with amphibole-bearing parageneses

Rock types with amphibole-bearing parageneses are widespread in the Odenwald. They belong to the calc alkaline intrusive suite (except for granites) or are amphibolites:

The fine-grained amphibolite of *sample 1,* with the assemblage hornblende-plagioclase-quartz-epidote-chlorite-biotite-ilmenite, is a typical wall rock of unit I, showing orientated growth of euhedral hornblende due to $D_{1/2}$. These amphibolites were intruded by gabbros and diorites of the Frankenstein pluton (TROCHIM, 1960)

UNIT	SAMPLE No.	ROCK TYPE (Field No.)	PARAGENESIS	Si/f.u. OF MUS	METHOD	P [kbar]	T [°C]	REMARKS
I	1	amphibolite (Kr84)	hbl-pl(An_{34})-qz-ep--chl-bi-ilm		8 9	1.5	545 530	deformed by $D_{1/2}$
I	2a	gabbro (K71)	2a/1:ol-cpx-opx-pl(An_{73})		5a,6 5b	1.5	880 930	intrusion depth undeformed
			2a/2: Ti-rich hbl_1-mt-ilm-sp 2a/3: Ti-poor hbl_2-talc-mt		7		690	$f(O_2)=10^{-17}$
	2b	pyroxene hornfels	pl(An_{50-70})-cpx-opx-qz-ilm-mt		5a 5b		900 975	data in Matthes & Schubert (1971)
I	3	granite vein (K55)	3/1: mus-bi-kf-pl(An_{10})-qz	3.045	4b	3.0	640	minimum intrusion depth; deformed at high temperature
			3/2: mus-ep-cc-chl-mt	3.100	4d	2.6	460	veinlet; retrograde mus
I	4	tonalite (Kr92)	4/1: hbl-pl(An_{35})-qz-tit--bi-ilm-mt 4/2: chl-ep-mus		8 9	2.4	545 550	undeformed
II	5	paragneiss (9836a)	bi-mus-gt-pl(An_{41})-qz-ilm		1	4.9	610	deformed by $D_{1/2}$ and D_3
II	6	metagabbro (Kr81)	cpx-pl(An_{47-63})-bi-hbl-ilm		9		700	deformed by D_3 magmatic cpx relics
II	7a	orthogneiss (Kr53)	bi-qz-kf-pl-sill-mus	3.035	4b	2.7	625	deformed by D_2; retrograde mus
	7b	gneiss	bi-qz-kf-pl-and/sill		11	2.0	600	observed by Okrusch et al. (1975)
II	8	kinzigite	8/1: gt_{core}-bi_1-pl_1(An_{53})		2 1	8.9	575 585	inclusions in garnet core
		(12148)	8/2: gt_{rim}-bi_2-pl_2(An_{42})-sill 8/3: mus-cord-bi_2-sill/and		1 3	4.3 2.5	610 600	matrix phases
II	9	orthogneiss/ HT-mylonite (Kr207)	9/1: gt_{core}-bi_2-mus_1--kf-pl(An_{18})-qz 9/2: bi-mus_2-kf-pl-qz	3.100 3.160	1 4a 4c	4.6 4.5 4.4	660 560	large magmatic muscovite deformed by D_3 recrystallized muscovite
II	10	orthogneiss/ HT-mylonite (Kr364)	10/1: bi-mus_1-kf-pl(An_{15})-qz 10/2: bi-mus_2-kf-pl-qz	3.110 3.110	4a 4c	4.7 3.8	 550	magmatic muscovite recrystallized muscovite deformed by D_3
II	11	granite (K70)	bi-mus-kf-pl(An_{11})-qz	3.035	4b	2.7	625	deformed by D_3 at T < 500°C
II	12	granite (Kr200)	bi-mus-kf-pl(An_{27})-qz	3.035	4b	2.7	625	deformed by D_3 at T > 500°C
II	13	granodiorite (9806)	hbl-bi-pl(An_{20})-kf-qz--tit-mt-ilm		10	3.0		intrusion depth; undeformed post-D_3 intrusion
III	14	granite vein (K91)	14/1: bi_1-mus_1-kf-pl(An_{12})-qz 14/2: bi_2-mus_2-kf-pl-qz	3.070 3.080	4a 4d	3.9 1.6	 450	depth of syn-D_4 intrusion pseudomorphs after cord or gt
III	15	migmatic gneiss (Kr133)	bi-mus-sill-kf-pl(An_{37})-qz	3.050	4b	3.2	645	retrograde mus
III	16	granodiorite (9788)	hbl-bi-pl(An_{23})-kf-qz--tit-ilm-mt		10	4.0		intrusion depth intruded during D_4
IV	17	biotite-plagioclase-gneiss (12588)	17/1: gt_1-bi_1-ky-pl(An_{26})-qz 17/2: gt_2-bi_2-mus-pl-qz-kf	 3.095	1 2 1 4a	8.6 7.8 4.8 4.6	805 763 620 650	bi,gt,ky as inclusions in plag matrix phases; deformed by $D_{1/2}$
IV	18	granitic mobilisate (K90)	bi-mus-qz-pl(An_{22})-kf	3.050	4b	3.2	645	formed on D_4 normal fault
IV	19	orthogneiss(K84)	bi-mus-qz-pl(An_{29})-kf	3.090	4a	4.4	650	deformed by $D_{1/2}$
IV	20	paragneiss (K80)	bi-mus-qz-pl-kf-sill	3.045	4b	3.1	640	retrograde muscovite
IV	21	gt-amphibolite (K84)	21/1: gt_{core}-ep_1-hbl_1-qz--pl(An_{94})-chl 21/2: cpx-pl(An_{22-29})-qz 21/3: hbl_2-pl(An_{29-46})-qz-bi--ilm 21/4: ep_2-cc-act-qz-chl		1	8.0	545	inclusions in garnet, $a_{H_2O}=1$ symplectite retrograde phases

Table 3. Geothermobarometric results. Mean P and T are given, the errors are represented in Fig. 3, mineral abbreviations in Table 4.

and	andalusite
bio	biotite
cc	calcite
chl	chlorite
cord	cordierite
cpx	clinopyroxene
ep	epidote
gt	garnet
hbl	hornblende
ilm	ilmenite
kf	K-feldspar
ky	kyanite
mt	magnetite
mus	muscovite
ol	olivine
opx	orthopyroxene
pl(Anx)	plagioclase with x mol% anorthite component
qz	quartz
sill	sillimanite
sp	spinel
tit	titanite

Table 4. Mineral abbreviations.

Sample 2a is an undeformed gabbro with the magmatic assemblage orthopyroxene-clinopyroxene-plagioclase-olivine occurring in unit I. Exsolution lamellae in the pyroxenes are extremely thin. Many pyroxenes and olivines are coated with a brown amphibole intergrown with green spinel, ilmenite and magnetite. Subsequently, green amphibole rims formed around pyroxenes and brown amphiboles. Talc and magnetite have grown along olivine-clinopyroxene contacts.

Sample 4 is a tonalite intrusive into unit I amphibolites. It is undeformed, and exhibits the magmatic assemblage hornblende-plagioclase-quartz-titanite-biotite-magnetite-ilmenite. However, abundant growth of xenoblastic epidote and chlorite and intensive sericitization of plagioclase cores suggest strong retrograde reequilibration.

Sample 6 is a foliated metagabbro from the southern part of unit II deformed by D_3. Oriented brownish green amphiboles grew across coarse relic magmatic pyroxene.

Sample 13 is a granodiorite occuring as NS-trending veins in the central part of unit II (HELLMANN, 1975), whereas *sample 16* was taken from a large granodioritic pluton in the northern part of unit III. The granodiorite occurrences crosscut D_3-structures. Both samples are undeformed, with a slightly porphyritic texture. Euhedral hornblende, titanite and plagioclase phenocrysts lie in a coarse quartz matrix in sample 16 and in a fine-grained quartz-feldspar matrix in sample 13. Both samples contain minor K-feldspar in the matrix. The cores of the zoned plagioclases are strongly sericitized and many magmatic biotites are chloritized along their margins.

Sample 21 is a garnet-amphibolite. This rock type occurs only in unit IV as small but abundant lenses in the gneisses. They were deformed by the early $D_{1/2}$-event together with the surrounding rocks. A detailed description was given by KNAUER et al. (1974). The garnet-amphibolite shows several prograde equilibration stages. Rounded garnets contain numerous inclusions of amphibole, clinozoisite, chlorite, biotite, K-feldspar-plagioclase-symplectites, anorthite, apatite, zircon, titanite and quartz. Inclusions of chlorite, biotite and clinozoisite were observed in mutual contact. The garnets are rimmed by a kelyphitic corona of plagioclase and plagioclase-hornblende-symplectites, while the matrix consists of clinopyroxene-plagioclase-quartz-symplectites overgrown by large xenoblastic amphiboles and biotite-quartz-symplectites. Actinolite, chlorite, calcite and epidote are late stage retrograde alteration products of hornblende, plagioclase and garnet.

5. Mineral chemistry

All mineral analyses were obtained with a CAMECA microprobe (Camebax). Operating conditions were 15 kV acceleration voltage, 14 nA sample current and 20 s measuring time, with a slightly defocussed beam in order to minimize alkali loss. Natural minerals (F-topaz, jadeite, rutile), as well as synthetic products (pure pyrope, pure spessartine, NaCl, Ba-silicate glass, Ca-Fe-silicate glass, K-silicate glass) were used as standards. Corrections were made using the PAP-program provided by CAMECA. The structural formulae of the mineral analyses, together with the method of recalculation are listed in tables 5 and 6.

Garnet: Due to variable bulk compositions of the garnet-bearing parageneses, garnet compositions vary from almandine-rich in the metapelitic samples 5, 8 and 17 (59–78 mol%) to spessartine-rich in the orthogneiss sample 9 (44 mol%) and grossular-rich compositions in the orthoamphibolite sample 21 (34 mol%). The garnet cores of samples 8, 17 and 21 have higher pyrope contents (13–19 mol%) compared to those of samples 5 and 9 (8–10 mol%). The pyrope content decreases in all samples from the core to the rim. The garnets of sample 17 that are broadly decomposed, are unzoned. The same is true for sample 9, where garnet is regarded as a magmatic phase. In both cases only the outermost rims of the garnets are influenced by retrograde metamorphism as shown for example by a clear increase in Mn-content. However, in sample 17 two types of unzoned garnet can be recognized: garnet enclosed in plagioclase shows a Fe to Fe+Mg ratio of 0.77, whereas garnet occurring as a matrix phase exhibits an Fe to Fe+Mg ratio of 0.84. Garnets from the other samples have a pronounced bell-shaped zoning. Sample 8 has a broad rim with an inverse zonation (Fig. 2), suggesting that core and rim represent two stages of garnet equilibration.

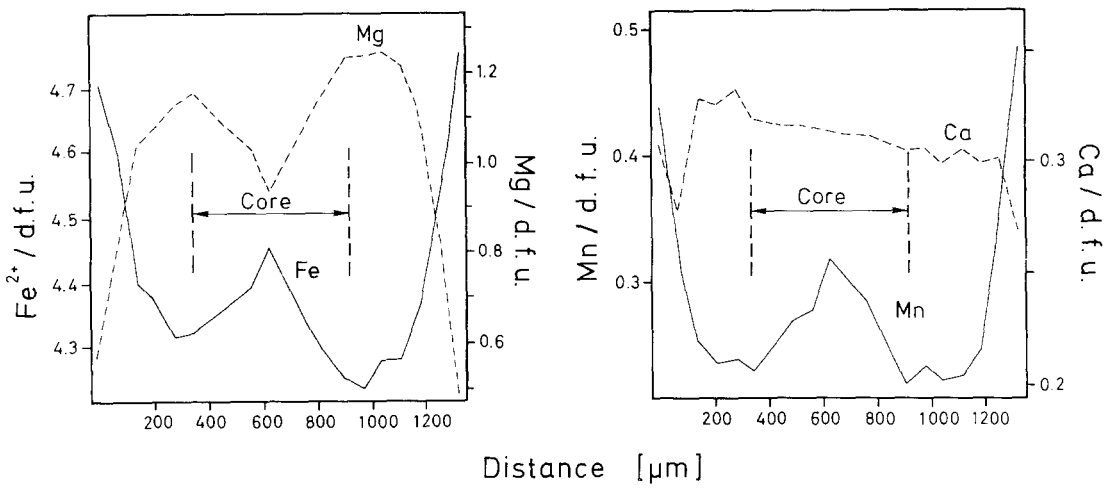

Fig. 2. Chemical zoning profiles of a garnet grain from the kinzigite sample 8 (d.f.u. = double formula unit).

Muscovite: All muscovites show a low celadonite component (3.03–3.16 Si p.f.u.) and Fe to Fe+Mg ratios > 0.5. Muscovite from sample 5 is exceptional, owing to a very high Ba-content (0.11 p.f.u.). Si-contents vary ± 0.01–0.02 p.f.u. around the mean composition, except in muscovites of samples 3 and 8 (retrograde muscovites of intermediate temperature). This variation of Si-contents is, however, within the analytical error. The paragonite components (3–10 mol% except 14 mol% in sample 8) and the fluorine contents (F/(F+OH) < 0.04) are low, and are assumed to cause a neglegible decrease or increase, respectively, of Si-contents.

Biotite: Biotites in samples of metapelitic and granitic composition show Mg to Mg+Fe ratios generally smaller than 0.5. However, this ratio is larger than 0.5 in biotites from mafic samples. Ti-contents are generally higher than 0.075 p.f.u.. Mn-contents are exceptionally high in retrograde biotites growing as pseudomorphs in granite sample 14. In the kinzigite sample 8, two types of biotite occur: biotite enclosed in garnet shows a Mg to Mg+Fe ratio of 0.65, whereas the biotite of the matrix exhibits a Mg to Mg+Fe ratio of 0.39.

Amphibole: All analysed amphiboles are calcic. Generally, they are magnesio-hornblendes as in the amphibolite samples 1 and 21, in granodiorite samples 13 and 16, and in the tonalite sample 4. All magnesio-hornblendes are similar in composition. In the undeformed olivine gabbro sample 2, two distinct hastingsitic amphiboles are found which differ markedly in Ti- and Cl-contents, as well as in Mg to Fe ratios. Hastingsitic amphibole can also be observed as inclusions in garnet of sample 21. The oriented, recrystallized amphiboles in metagabbro sample 6 are pargasitic.

Pyroxene: The pyroxenes in the olivine gabbro sample 2 are augite and bronzite, while those in samples 6 and 21 are salites.

Chlorite: The analysed chlorites generally plot in the pycnochlorite/Mg-rhipidolite field. Only chlorite found as inclusions in garnets of sample 21 are Mg- and Si-rich (pennine).

Plagioclase: Plagioclase compositions are given in Table 3. Contents of anorthite vary from 10 to 29 mol% in granitoids, 26 to 42 mol% in metapelitic rocks and 34 to 73 mol% in intermediate to mafic assemblages. In kinzigite sample 8 anorthite contents of plagioclase inclusions in garnets (53 mol%) differ from those of the matrix (42 mol%). In the garnet-amphibolite sample 21 three different plagioclase generations can be distinguished: Plagioclase inclusions contain 94 mol% anorthite, those in clinopyroxene-quartz-plagioclase symplectites 22–29 mol% and plagioclase in the coronas around garnet 29–46 mol%.

Epidote: The compositions of the analysed epidotes vary between 61–86 Mol % pistacite.

6. Derivation and discussion of the PT-paths

The results of the geothermobarometric methods applied are listed in Table 3 and were used to construct the PT-paths of Fig. 3. The estimated PT error bars shown result from a combination of analytical uncertainties and errors inherent in the methods used. The four paths differ considerably, because four successive deformation

Muscovite
Ions based on 44 valencies

Sample/ Paragenesis	3/1	3/2	5	7	8	9/1	9/2	10/1	10/2	11
Si	6.093	6.174	6.400	6.074	6.102	6.201	6.332	6.214	6.222	6.074
Al^{IV}	1.907	1.826	1.600	1.926	1.898	1.799	1.668	1.786	1.778	1.926
Al^{VI}	3.600	3.409	3.655	3.761	3.820	3.530	3.356	3.612	3.581	3.751
Ti	0.053	0.077	0.002	0.059	0.023	0.047	0.070	0.017	0.027	0.006
Cr	0.002	0.000	0.000	0.001	0.000	0.001	0.000	0.001	0.000	0.000
Fe^{2+}_{tot}	0.386	0.487	0.112	0.121	0.099	0.404	0.440	0.316	0.330	0.337
Mn	0.002	0.002	0.014	0.001	0.001	0.004	0.004	0.004	0.002	0.005
Mg	0.077	0.176	0.191	0.109	0.105	0.125	0.241	0.145	0.163	0.037
Ca	0.000	0.000	0.061	0.000	0.000	0.000	0.000	0.000	0.000	0.000
Ba	0.002	0.001	0.234	0.010	0.001	0.001	0.003	0.004	0.000	0.001
Na	0.142	0.070	0.125	0.135	0.273	0.096	0.063	0.086	0.105	0.123
K	1.816	1.888	1.701	1.792	1.661	1.856	1.880	1.856	1.830	1.767
F	0.012	0.090	0.032	0.005	0.026	0.026	0.045	0.038	0.067	0.045
Cl	0.003	0.000	0.002	0.001	0.000	0.001	0.003	0.000	0.001	0.002
OH	3.986	3.910	3.966	3.994	3.974	3.973	3.952	3.962	3.931	3.953
n	11	1	5	7	1	7	5	6	5	6

	12	14/1	14/2	15	17	18	19	20
Si	6.072	6.163	6.104	6.104	6.192	6.098	6.186	6.089
Al^{IV}	1.928	1.837	1.896	1.896	1.808	1.902	1.814	1.911
Al^{VI}	3.793	3.693	3.674	3.674	2.962	3.469	3.331	3.577
Ti	0.027	0.010	0.049	0.049	0.284	0.117	0.115	0.084
Cr	0.002	0.001	0.003	0.003	0.008	0.001	0.002	0.003
Fe^{2+}_{tot}	0.131	0.229	0.226	0.226	0.368	0.397	0.505	0.336
Mn	0.003	0.009	0.002	0.002	0.006	0.001	0.004	0.002
Mg	0.101	0.171	0.131	0.131	0.368	0.125	0.199	0.119
Ca	0.000	0.000	0.000	0.000	0.000	0.000	0.000	0.000
Ba	0.014	0.004	0.008	0.008	0.009	0.001	0.014	0.019
Na	0.157	0.115	0.090	0.090	0.090	0.102	0.095	0.205
K	1.766	1.775	1.831	1.831	1.755	1.884	1.823	1.685
F	0.013	0.166	0.041	0.041	0.029	0.052	0.029	0.000
Cl	0.001	0.000	0.001	0.001	nd	0.002	0.002	0.001
OH	3.985	3.834	3.957	3.957	3.971	3.945	3.969	3.999
n	8	10	5	5	1	6	10	5

Table 5. Mean structural formula (double formula units) of analysed a) muscovite b) biotite.

phases between 410 and 330 Ma disturbed the thermal structure of the crust locally to a different extent.

Unit I

A high early geotherm of at least 70°–80°C/km is indicated from the data determined from amphibolite sample 1. These data appear to be realistic because subsequent gabbroic intrusions of the Frankenstein pluton were emplaced at the same crustal level, corresponding to 1–2 kbar (sample 2a). Such a shallow depth of intrusion was already inferred by TROCHIM (1960), MATTHES & SCHUBERT (1971) and KIRSCH et al. (1988). During early cooling, hastingsite-magnetite-ilmenite symplectites formed in the gabbro at 690°C and an O_2-fugacity near the magnetite-hematite-buffer. Equilibration temperatures of pyroxene hornfelses (sample 2b) at the immediate contact to the gabbro are similar to those of the gabbro solidus at 900°C. Formation of a secondary low-Ti-amphibole in the gabbro occurred at a later stage during cooling. Its chemical composition is typical for temperatures around the amphibolite/greenschist facies transition according to RAASE (1974). These temperatures would correspond to the temperatures inferred for the concomitant regional metamorphism.

In both amphibolites and gabbros, discrete shear planes with D_3-kinematics are found with recrystallized amphibole and plagioclase (KROHE, 1991b). This indicates that temperatures > 500°C persisted in unit I after emplacement of the Frankenstein pluton.

A granite vein (sample 3) that intruded the Frankenstein gabbro yields a minimum intrusion

	Biotite									
	Ions based on 44 valencies									
Sample/ Paragenesis	1	4	5	6	7	8/1	8/2	9	12	13
Si	5.587	5.571	5.376	5.554	5.246	5.388	5.273	5.595	5.267	5.615
Al^{IV}	2.413	2.429	2.624	2.446	2.754	2.612	2.727	2.405	2.733	2.385
Al^{VI}	0.444	0.424	0.643	0.506	0.906	0.714	0.851	0.707	0.803	0.308
Ti	0.188	0.199	0.258	0.152	0.239	0.185	0.274	0.304	0.269	0.204
Cr	0.019	0.000	0.007	0.000	0.000	0.000	0.013	0.000	0.005	0.022
Fe_{tot}	2.023	2.602	2.842	2.402	2.761	1.671	2.805	2.503	2.787	2.256
Mn	0.020	0.036	0.128	0.041	0.057	0.016	0.009	0.036	0.035	0.039
Mg	3.142	2.605	2.036	2.744	1.758	3.163	1.770	2.086	1.798	3.091
Ca	0.006	0.010	0.002	0.019	0.000	0.000	0.000	0.000	0.000	0.007
Ba	0.007	0.017	0.008	0.011	0.000	0.008	0.012	0.000	0.008	0.004
Na	0.018	0.023	0.046	0.010	0.037	0.201	0.046	0.017	0.043	0.011
K	1.859	1.799	1.800	1.875	1.897	1.606	1.804	1.797	1.914	1.834
F	0.049	0.071	0.040	0.118	0.206	0.103	0.000	0.352	0.096	0.298
Cl	0.021	0.010	0.016	0.000	0.029	0.000	0.034	0.012	0.037	0.019
OH	3.930	3.918	3.944	3.882	3.769	3.897	3.966	3.636	3.867	3.683
n	1	1	4	1	1	1	1	1	3	3

	14/1	14/2	15	16	17/1	17/2	18	20	21/3
Si	5.517	5.441	5.243	5.566	5.313	5.390	5.342	5.305	5.435
Al^{IV}	2.483	2.559	2.757	2.434	2.687	2.610	2.658	2.695	2.565
Al^{VI}	1.109	1.040	0.713	0.260	0.759	0.666	0.589	0.697	0.127
Ti	0.235	0.167	0.297	0.321	0.318	0.326	0.417	0.281	0.545
Cr	0.002	0.002	0.007	0.000	0.012	0.036	0.002	0.001	0.005
Fe_{tot}	2.889	2.846	2.995	2.535	2.383	2.340	2.760	2.392	2.542
Mn	0.077	0.236	0.055	0.044	0.036	0.036	0.054	0.044	0.007
Mg	1.213	1.362	1.619	2.680	2.161	2.313	1.825	2.342	2.467
Ca	0.000	0.000	0.000	0.000	0.000	0.000	0.003	0.000	0.004
Ba	0.000	0.000	0.000	0.044	0.013	0.000	0.000	0.005	nd
Na	0.009	0.017	0.030	0.029	0.062	0.058	0.035	0.055	0.019
K	1.844	1.879	1.972	1.819	1.856	1.857	1.909	1.859	1.938
F	0.425	0.383	0.189	0.154	0.050	0.058	0.085	0.097	nd
Cl	nd	nd	0.021	0.011	nd	nd	0.011	0.007	nd
OH	3.575	3.617	3.790	3.835	3.950	3.942	3.904	3.896	4.000
n	3	8	2	1	1	1	3	3	2

Table 5. continued n number of samples; nd not determined

depth corresponding to a pressure of 3 kbar. This value is significantly different from the maximum possible intrusion depth of the older gabbroic intrusion. Retrograde muscovite in the same sample equilibrated under low-grade conditions at pressures of 2–3 kbar. This pressure is independently corroborated by data from the retrograde equilibration of the tonalite sample 4.

Hence, unit I must have subsided during emplacement of the calc alkaline intrusive suite. An anticlockwise PT-path results for unit I with an early high geotherm of 70°–80°C/km decreasing during subsidence. Therefore, it is not surprising that hornblende cooling ages in this unit are the oldest in the Odenwald.

Unit II

Mineral relics yielding informations about the prograde branch of the PT loop for unit II are scarce. Only the kinzigite sample 8 of unit II provides data from minerals enclosed in garnet. The pertaining PT-data calculated under consideration of garnet core compositions indicate PT-conditions around 580°C/9 kbar, typical for the amphibolite/eclogite facies transition. However, it must be noted that the lens containing the kinzigites, as well as the surrounding granitoids and metapelites, are overprinted by NE-SW-trending zones of D_3-strike shear that are abundant in unit II (Krohe 1991b). Hence this lens with its relics indicative of higher pressures can be regarded as relatively allochthonous with respect to other rocks of unit II at an early stage of crustal history.

In the metapelites of the »Heppenheimer Schieferzug« in the southern part of unit II, rocks have undergone dehydration mineral reactions and no relics were detected (see von Raumer, 1973). Peak PT-conditions of 595°C and 5 kbar have been

Garnet Ions based on 24 valencies										
Sample/ Paragenesis	5 C	5 R	8 C	8 R	9 C	9 R	17/1	17/2	21 C	21 R
Si	2.973	2.979	2.931	2.937	3.005	3.004	2.992	2.970	2.958	2.988
Al	1.990	1.986	2.013	1.987	1.957	2.021	1.989	1.992	1.987	1.970
Ti	0.002	0.002	0.004	0.010	0.012	0.000	0.001	0.002	0.006	0.008
Fe^{2+}_{tot}	2.203	2.298	2.184	2.389	1.387	1.237	1.807	1.814	1.728	1.750
Mn	0.300	0.283	0.137	0.232	1.328	1.529	0.586	0.797	0.130	0.043
Mg	0.319	0.231	0.594	0.303	0.255	0.178	0.519	0.334	0.393	0.285
Ca	0.239	0.281	0.138	0.142	0.086	0.050	0.122	0.120	0.853	1.072

C Core composition; R Rim composition; representative analyses

Pyroxene 4 cations per 6 oxygens				
Sample	2 Cpx	2 Opx	6 Cpx	21 Cpx
Si	1.900	1.938	1.958	1.954
Al^{IV}	0.100	0.062	0.032	0.046
Al^{VI}	0.030	0.006	0.004	0.021
Ti	0.021	0.004	0.009	0.001
Fe^{3+}	0.055	0.048	0.039	0.064
Fe^{2+}	0.179	0.408	0.308	0.268
Mn	0.007	0.012	0.016	0.006
Mg	0.816	1.490	0.636	0.684
Ca	0.860	0.032	0.974	0.914
Na	0.032	0.000	0.014	0.042
n	3	3	5	6

nd not determined; n number of samples

Sample/ Paragenesis	Ilmenite 2a/2	Magnetite	Spinel
Al	0.000	0.032	1.917
Cr	0.001	0.039	0.032
Ti	0.964	0.098	0.005
Fe^{3+}	0.000	1.735	0.046
Fe^{2+}	0.975	1.076	0.530
Mn	0.039	0.005	0.007
Mg	0.055	0.015	0.432
Zn	0.000	0.002	0.044
O	5.000	4.000	4.000
n	3	1	2

Sample	Staurolite 8	Cordierite
Si	7.442	4.949
Al	18.523	4.036
Ti	0.194	0.000
Fe^{2+}	2.836	0.907
Mn	0.029	0.025
Zn	0.509	0.000
Mg	0.466	1.082
Na	0.000	0.052
H	2.204	0.000
O	48.000	18.000
n	1	1

Table 6. Mean structural formula of analysed a) garnet, pyroxene, spinel, ilmenite, magnetite, staurolite and cordierite; b) amphibole, epidote and chlorite.

derived for sample 5, which are similar to those calculated for garnet rim and matrix biotite compositions of the kinzigite. These are compatible with earlier PT-estimations based on the upper stability of cordierite + muscovite and the evaluation of garnet-cordierite-pairs (OKRUSCH et al., 1975). Maximum temperatures of about 650°C are indicated by the local occurrence of anatectic mobilisates that are only found in the southern part of unit II.

Samples 9 and 10 are mylonitic granite gneisses which were affected by D_3-shearing in the northern part of unit II at a relatively early stage of the D_3-event (HUSTIAK & KROHE, 1990). The intrusion depths of the magmatic protolith corresponding to about 4–5 kbar were determined by methods 1 and 4a. Muscovites which recrystallized during solid state deformation formed at pressures between 3.6 and 4.5 kbar.

In contrast to the above, granitoids, which intruded synkinematically with respect to D_3 (samples 11 and 12) were emplaced at a shallower level corresponding to $\geq$ 2.7 kbar in the central area of unit II. These minimum intrusion depths may be close to the actual values, because the intersection of the Si-isopleths with the muscovite + quartz-breakdown curve is near the intersection of the latter with the wet granite solidus. Both granites were deformed on cooling below (sample 11) and above (sample 12) temperatures of 500°C, which are required for plastic deformation of feldspar.

The mafic intrusions of unit II were also de-

	Amphibole Ions based on 46 valencies; 13 cations except Ca,Na,K								
Sample/ Paragenesis	1	2a/2	2a/3	4	6	13	16	21/1	21/2
Si	6.97	6.17	6.21	6.69	6.24	6.71	6.59	6.12	6.52
Al^{IV}	1.03	1.83	1.79	1.31	1.76	1.29	1.41	1.88	1.48
Al^{VI}	0.11	0.32	0.57	0.14	0.51	0.08	0.16	0.50	0.38
Ti	0.11	0.23	0.02	0.18	0.15	0.15	0.11	0.13	0.09
Cr	0.01	0.01	0.00	0.00	0.00	0.00	0.00	0.00	0.01
Fe^{3+}	0.68	0.45	0.74	0.62	0.23	0.58	0.72	0.56	0.60
Fe^{2+}	0.96	0.75	1.50	1.45	2.19	1.33	1.59	2.16	1.45
Mn	0.04	0.01	0.03	0.06	0.05	0.05	0.06	0.01	0.02
Mg	3.09	3.23	2.13	2.54	1.87	2.79	2.35	1.63	2.46
Ca	1.84	1.89	1.92	1.84	1.99	1.87	1.85	1.95	1.88
Na^{M4}	0.16	0.11	0.08	0.16	0.01	0.13	0.15	0.05	0.12
Na^{A}	0.11	0.53	0.46	0.21	0.48	0.27	0.24	0.43	0.26
K	0.06	0.17	0.05	0.13	0.26	0.17	0.21	0.17	0.17
F	0.04	0.05	0.01	0.03	0.06	0.16	0.10	nd	nd
Cl	0.02	0.01	0.06	0.02	0.00	0.04	0.02	nd	nd
OH	1.94	1.95	1.92	1.92	1.94	1.80	1.88	2.00	2.00
n	6	6	3	8	6	5	6	2	8

	Epidote Ions based on 50 valencies					Chlorite Ions based on 56 valencies				
Sample/ Paragenesis	1	3/2	4/2	21/1	21/3	1	3/2	4/2	21/1	21/3
Si	6.10	5.98	6.02	5.94	5.94	5.64	5.21	5.54	6.80	5.57
Al^{IV}	0.00	0.00	0.00	0.00	0.00	2.36	2.79	2.46	1.20	2.43
Al^{VI}	4.12	4.44	4.75	4.87	4.41	2.30	2.59	2.44	1.39	2.26
Ti	0.00	0.01	0.00	0.04	0.01	0.04	0.01	0.01	0.01	0.00
Fe^{3+}	1.72	1.54	1.24	1.22	1.67	0.00	0.00	0.00	0.00	0.00
Fe^{2+}	0.00	0.00	0.00	0.00	0.00	2.98	5.33	4.05	2.25	4.72
Mn	0.02	0.02	0.01	0.01	0.05	0.06	0.09	0.09	0.01	0.04
Mg	0.00	0.00	0.00	0.00	0.00	6.56	4.06	5.36	8.20	5.05
Ca	3.99	4.03	3.93	3.89	3.94	0.04	0.01	0.01	0.03	0.01
Na	0.00	0.00	0.00	0.00	0.00	0.00	0.00	0.00	0.01	0.00
K	0.00	0.00	0.00	0.00	0.00	0.04	0.00	0.00	0.00	0.00
F	0.00	0.00	0.00	0.00	0.00	0.00	0.00	0.01	0.00	0.00
Cl	0.00	0.00	0.00	0.00	0.00	0.00	0.01	0.00	0.01	0.01
OH	2.00	2.00	2.00	2.00	2.00	16.00	15.99	15.99	15.99	15.99
n	4	8	4	1	1	1	1	2	1	1

Table 6. continued

formed synkinematically with D_3 (KROHE, 1991b), because oriented growth of pargasitic amphiboles in the strongly deformed metagabbro sample 6 already occurred at 700°C.

The undeformed granodiorite sample 13 in the central part of unit II intruded postkinematically with respect to D_3, because it occurs in NNW-SSE-trending veins cutting the s_3-foliation (HELLMANN, 1975), and because it shows a late K/Ar hornblende cooling age of 330 Ma (HELLMANN et al., 1982). The intrusion depth of 3 kbar was obtained by method 10 and is an independent corroboration of pressures obtained by phengite barometry from samples 11 and 12. Hence, it is assumed that the entire unit was situated at a crustal level corresponding to 3 kbar at the end of D_3, below the temperature of the brittle/ductile deformation transition for feldspars.

In contrast to the northern part of unit II, a different retrograde path with a rather strong increase of the geotherm can be observed in the southern part of unit II. This is indicated by PT-data obtained from retrograde muscovite grown across sillimanite (sample 7a) and the breakdown of muscovite + quartz to andalusite + K-feldspar and sillimanite + K-feldspar, respectively (OKRUSCH et al., 1975). However, stable muscovite also exists in this area; hence local muscovite + quartz-breakdown could be due to variation in water activity. The late increase of the geotherm may be due either to rapid uplift in the south relative to the north during D_3 or D_4 or due to isobaric heating. At the

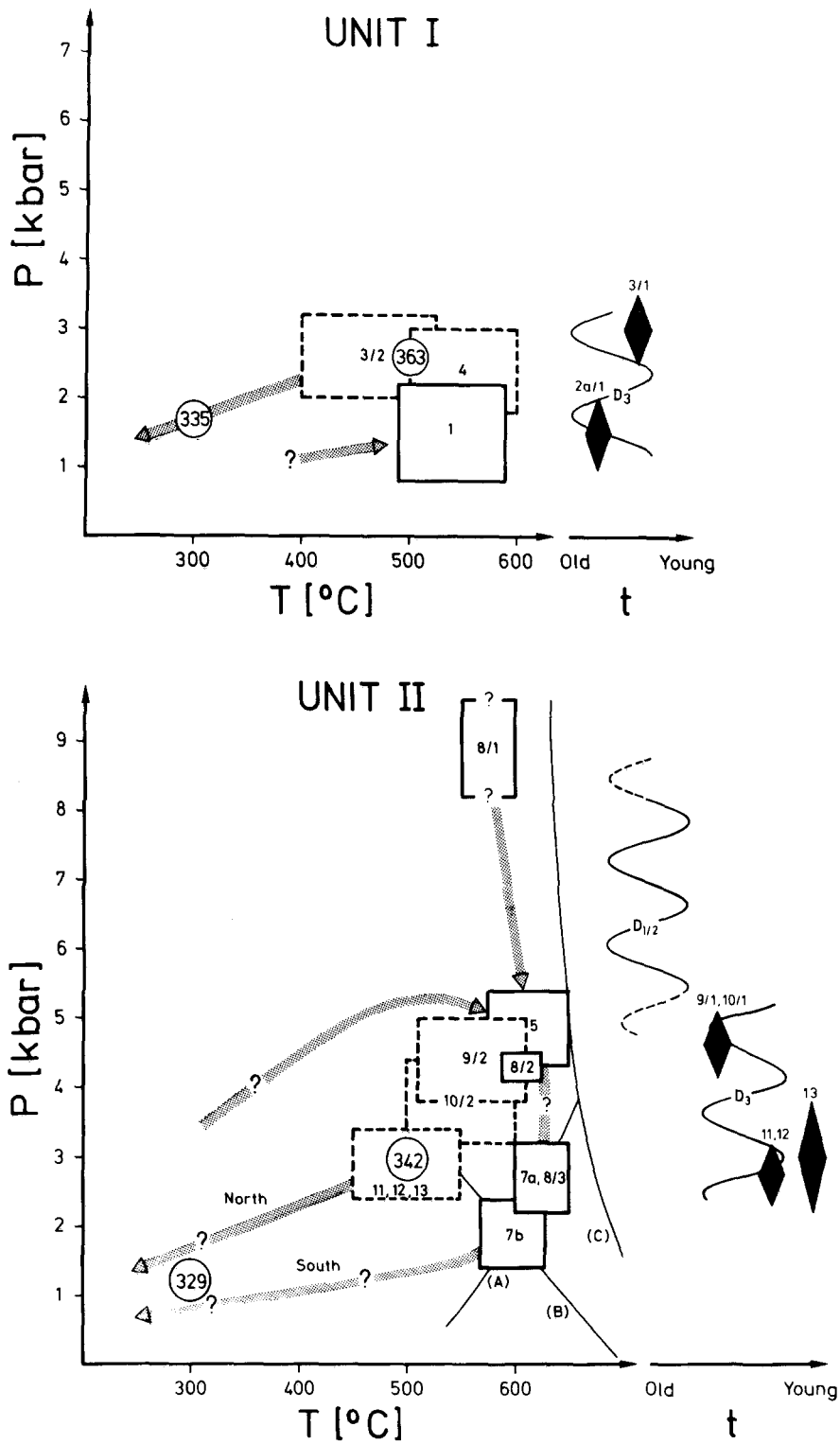

Fig. 3. PT-paths for the different crustal units of the Odenwald. Boxes with solid lines represent mean PT-data determined from metamorphic rocks with estimated errors; boxes with broken lines represent retrograde PT-data determined from plutonic rocks after cooling to temperatures prevailing in the respective crustal section. Diamonds indicate pressures with estimated errors corresponding to intrusion depths. Numbers in boxes and beside diamonds refer to the sample/paragenesis (see Table 1). Wavy lines show deformation phases. Mean K/Ar hornblende and biotite cooling ages from KREUZER & HARRE (1975), RITTMANN (1984), LIPPOLT (1986) and KIRSCH et al. (1988) are shown in circles. A U/Pb zircon cooling age of TODT (1979) is included. Lines indicated by A, B and C refer to the muscovite + quartz breakdown curve of CHATTERJEE & JOHANNES (1974), the andalusite-sillimanite transition curve of HOLDAWAY (1971), and the wet granite solidus of JOHANNES (1984), respectively.

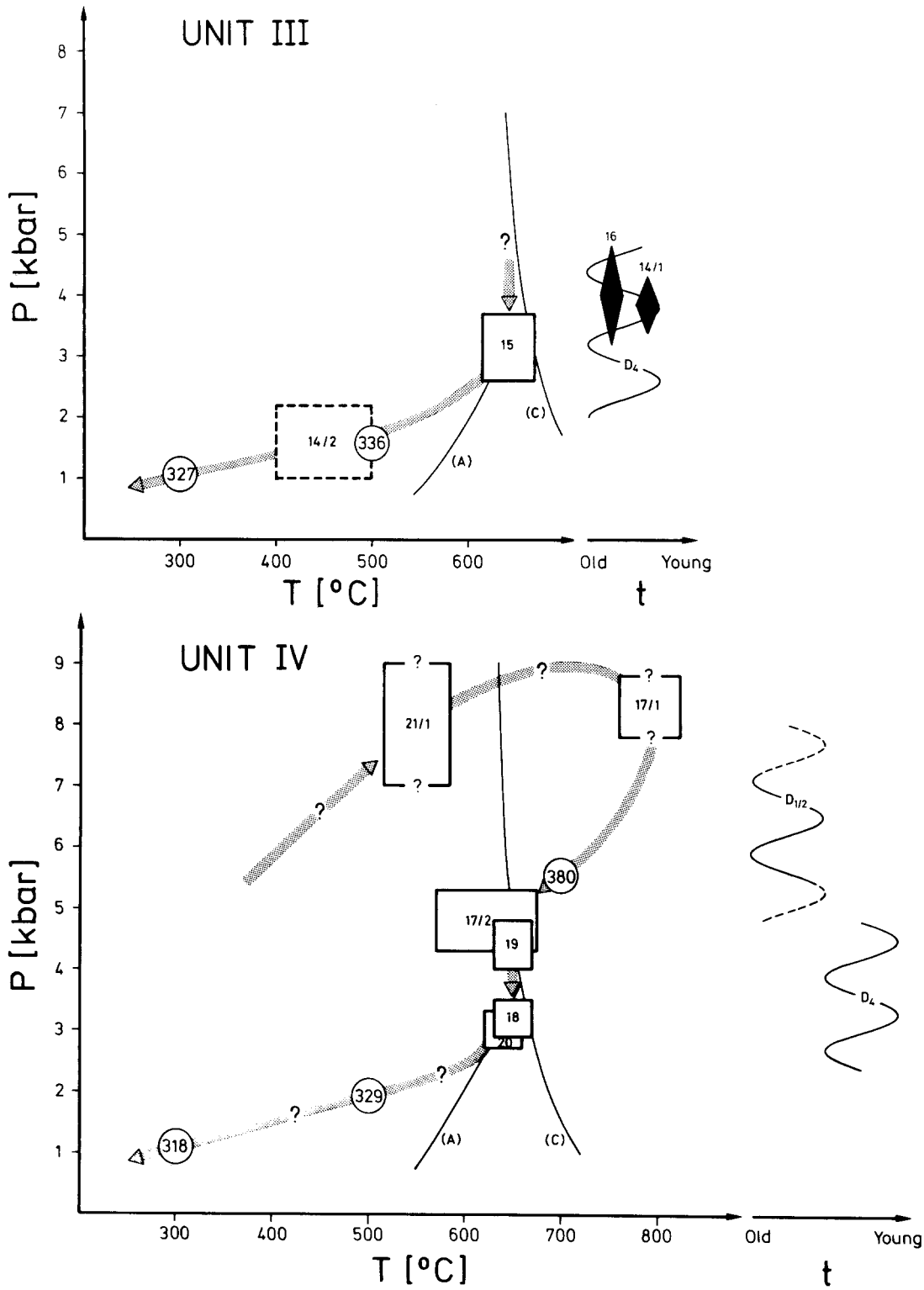

moment, no conclusive interpretation can be given.

Unit III

Prograde and metamorphic peak PT-data for unit III are not yet available. Uplift in zone III is related to the D_4 extensional event, causing a penetrative foliation along the border zones (Krohe, 1991a). Voluminous granitoid bodies of unit III show intrusion depths corresponding to pressures of 4 kbar (samples 14 and 16). However, the mineral data from units II and III are significantly dif-

ferent and support the observed pressure difference of 1 kbar during granitoid intrusions between both units. The intrusions of unit III show lower K/Ar hornblende cooling ages (333–337 Ma) than those of unit II (340–344 Ma; KREUZER & HARRE, 1975; RITTMANN, 1984). Intrusions of unit III during the D_4-event are also indicated by the structures (KROHE, 1991a). Hence the granitoids of unit III are younger than those of unit II at the end of D_3, which, however, seem to be emplaced at a shallower crustal level.

Retrograde PT-data determined for granitoids and wall rocks of unit III (samples 14 and 15) indicate nearly isothermal, i.e. rapid uplift. The geotherm increased to about 60°–80°C/km.

The change of the PT-paths from unit II to unit III correlates with a change in the tectonic regime from normal, oblique strike-slip D_3 to normal faulting D_4. In unit III, granitoids were affected by normal faults (D_4) that developed at different stages during the cooling history, involving both plastic and brittle deformation mechanisms of quartz and feldspar (KROHE, 1991a).

Unit IV

The two samples 17 and 21 provide information about the prograde branch of the PT-path of unit IV. Calculated PT-conditions for the garnet-amphibolite sample 21 using garnet core inclusions lie in the PT-range of 545°C/8 kbar, which are typical for the amphibolite/eclogite facies transition. These results are similar to those of garnet core formation in the kinzigites of unit II. Sample 21 shows breakdown of garnet to kelyphitic coronas and formation of clinopyroxene-plagioclase-symplectites, possibly from an amphibole precursor at granulite conditions.

Calculated PT-data considering inclusions in the metaacidite sample 17 indicate heating of this rock up to 800°C at pressures between 7 and 9 kbar. Because garnet amphibolites are fairly widespread over unit IV (KNAUER et al., 1974), it is assumed that most rocks of this unit had a granulitic precursor before being rehydrated during emplacement into shallower crustal levels by $D_{1/2}$. Granulite-facies conditions dominated before and possibly during the $D_{1/2}$-episodes.

PT-conditions of about 4.5 kbar/650°C for the static equilibration after $D_{1/2}$ under wet conditions were obtained from samples 17 and 19. These PT-data are similar to the peak PT-conditions of unit II. Anatectic phenomena at that stage are abundant in the entire unit. Due to widely varying chemical compositions of plagioclase and amphibole no reliable PT-datum for this stage could be derived from the garnet-amphibolite (sample 21).

Further uplift after amphibolite facies equilibration is mainly controlled by the D_4-extensional tectonics causing the dominant NNE-SSW trending antiform structure and a broad zone of mylonites at the western border of unit IV (»Otzberg zone«). These mylonites show normal-fault kinematics; deformation continued during cooling showing recrystallization over the temperature range of 300°–600°C (KROHE, 1991a). Anatectic mobilisates on D_4-normal fault planes (sample 18) indicate that D_4 began at high temperatures. Equilibration took place at 3.2 kbar, as shown by the data for early, retrograde muscovite growth (sample 20). This suggests an isothermal uplift corresponding to a pressure difference of about 1.5 kbar during D_4, similar to that of unit III. Local muscovite + quartz breakdown probably due to lowering of water activity and subsequent rehydration as in sample 20, is more rarely observed in unit IV as compared to units II and III.

7. A model for crustal dynamics in the Odenwald area

The PT-paths reflect episodes of burial and uplift of crustal slices, i.e. tectonic events involving prominent vertical displacements at rapid rates. In the Odenwald, distinct compressional and extensional tectonic events associated with large vertical components of relative displacements have been inferred from regional structures and microstructures (KROHE, 1991a, b). The tectonic events correlate with the prograde and retrograde branches of the PT-paths. Available geochronologic data and the very limited stratigraphic record allow a correlation of the tectonic evolution with time and with the corresponding sections of the PT-paths.

The prograde branch of the PT-loops

The limited information on the prograde PT-paths indicates that at least some of the metamorphic rocks of units II and IV equilibrated in the lower crust – probably under granulite facies conditions – before being rehydrated under amphibolite facies conditions. The prograde path reflected by the three samples 8, 17 and 21 for unit IV, and a small lens in unit II, is interpreted here as

due to rapid burial and subsequent nearly isobaric heating at lower crustal pressure conditions. In other parts of the Odenwald area, metamorphic rocks seem to have experienced only dehydration reactions towards peak amphibolite facies conditions, without medium-pressure relics. Hence before or during the thermal peak of the amphibolite facies metamorphism, rocks from the uppermost crustal levels and from the lower crust must have been juxtaposed in intermediate crustal levels by an early tectonic event. Structures related to this compressive event involving crustal stacking ($D_{1/2}$) are the oldest preserved deformational structures (KROHE, 1991a).

However, there is no strict correlation between the PT conditions obtained from the inclusion phases and the early stages of the deformation history. The microstructures that are related to the oldest deformation episodes ($D_{1/2}$) annealed during amphibolite facies metamorphism. They developed in the time-span between the granulite facies metamorphism and the thermal peak of the amphibolite facies metamorphism. In unit II, early deformational microstructures frozen in during the thermal peak of amphibolite facies metamorphism have been described by HUSTIAK & KROHE (1990).

The age of the compressive $D_{1/2}$-event can be bracketed between 420 and 360 Ma as follows. The maximum age is given as Ludlovian, the only biostratigraphically controlled age for metasediments in the Mid-German Crystalline Rise, found within schists in the nearby Spessart (PFLUG & REITZ, 1987). The minimum age is given by the oldest K/Ar hornblende cooling ages because the deformation ceased before or at the thermal peak of metamorphism. A discordant U/Pb age of 380 Ma by TODT (1979) within metasediments of unit IV was interpreted as an age of metamorphism. It may reflect the age of cooling under the 700°C-isotherm in that region and hence roughly indicates the age of the $D_{1/2}$-event.

The thermal peak of amphibolite facies metamorphism

In units II and IV, »peak« PT-conditions at about 4–5 kbar and 600–650°C reflect a slightly increased geotherm of 35°–40°C/km with respect to a »normal« geotherm. This may be due to concomitant calcalkaline intrusions (orthogneisses in unit IV and northern unit II; amphibolites?). At present, the crust has a normal thickness of about 28 km in the Odenwald area (DEKORP RESEARCH GROUP, 1985). This suggests an excess crustal thickness (40 km at least) before the onset of the D_3-and D_4-events which controlled the uplift.

In unit I the peak amphibolite facies conditions indicate an exceptionally high initial geotherm of 70°–80°C/km. This geotherm may be prekinematic. Thus unit I, which is dominated by amphibolites, could represent oceanic or rifted continental marginal crust, where such geotherms are typical. During later crustal history, the geotherm in unit I decreased to the prevailing regional one.

The occurrence of rocks exposed at present that have equilibrated at different crustal levels during the peak of amphibolite facies metamorphism is explained by vertical components of displacement associated with two deformational events after the thermal peak.

Uplift during transtensional movements D_3

Unit II and to a lesser extent unit I were affected by D_3. During this event, steep NE-SW trending shear zones developed that are characterized by sinistral strike-slip and a normal-fault component (»transtension« KROHE, 1991b; Fig. 4).

Within unit II, normal faulting associated with D_3 caused a relative uplift of the marginal parts of unit II with respect to the central parts of unit II (KROHE, 1991b). This is in accordance with the PT-data of the synkinematic granites, because those rocks in marginal parts of unit II suffered from a decrease in pressure from 4.5 to 3.5 kbar during mylonitisation, while those in the central parts reflect isobaric cooling and mylonitisation at 3 kbar.

The PT-data imply large, vertical relative displacements between units I and II associated with the D_3-event, possibly along a northward dipping fault zone between both units (KROHE, 1991a):

While the synkinematic calcalkaline suite intruded at depths corresponding to 2.7–4.7 kbar during uplift of unit II, intrusion depths were generally shallower in unit I at the same time, i.e. 1.5–3 kbar. During D_3 unit I must have subsided, as shown by the anticlockwise PT-path obtained for unit I. At the end of D_3 units I and II were situated at the same depth, corresponding to 3 kbar. The age of the D_3-event may be bracketed between at least 363 Ma (age of the oldest intrusion according to KIRSCH et al. 1984) and about 342 Ma, as the closing temperature of the mean K/Ar-hornblende cooling ages (KREUZER & HARRE, 1975; RITTMANN, 1984) is identical to the temperature of the brittle/ductile deformation transition of feldspar.

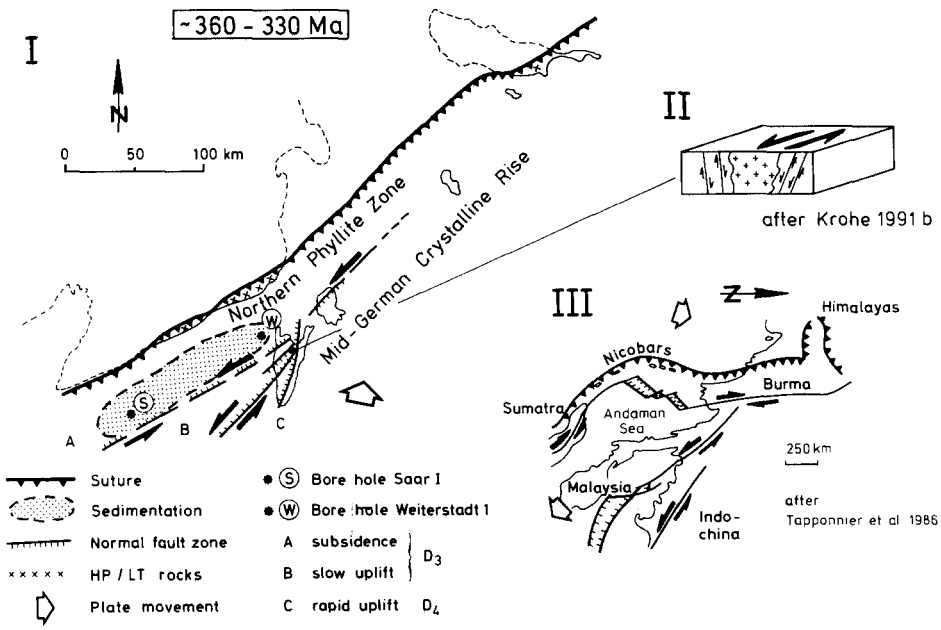

Fig. 4. I – Sketch of paleogeographic elements in the Mid-German Crystalline Rise during the period 360–330 Ma; II – sketch of the transtensional setting of the central Odenwald; III – the Burma/Sumatra collision zone as a recent model for the Mid-European Variszides. For better comparison the NS-orientation was rotated 90° clockwise.

The relative vertical displacements between unit I and II are compatible with stratigraphic data at still shallower crustal levels. In the extension of the subsiding unit I toward the SW, sediments from at least one of two relevant bore cores (Fig. 4I) indicate concomitant deposition. At borehole Saar I (see ZIMMERLE et al., 1976) continuous Upper Devonian-Lower Carboniferous sediments were deposited from Mid-Givetian onward on top of an 381 Ma old exhumed undeformed granite (LENZ & MÜLLER, 1976). At Weiterstadt 1 (MARELL, 1989) sedimentation probably began during the Visean on top of a basement of amphibolites, because the Ar^{39}/Ar^{40} biotite age of a basaltic layer above these lowermost sediments yielded 332 Ma (KIRSCH, 1984).

Retrogression during the D_4-event

Within unit III, D_4-normal faulting on NNE-SSW trending, WNW dipping planes suggest relative uplift of the southeastern parts with respect to the northwestern region. Between unit IV and unit III a WNW-dipping D_4-shear zone with normal fault geometry suggests uplift of unit IV relative to unit III (KROHE, 1991a). In addition, KROHE (1991a) infers a larger vertical component of displacement compared to the D_3-structures.

The PT-data of rocks affected by the D_4-event in units III and IV reflect more rapid and greater uplift relative to the north-western parts of the Odenwald due to normal faulting. This is shown by a greater intrusion depth of granitoids synkinematic to D_4 relative to the older intrusions of unit II. The retrograde branches of the PT-paths of units III and IV are characterized by isothermal uplift and hence a very strong increase of the geotherm to about 60°–80°C/km. A similar path is detectable in the southern part of unit II.

These late, rapid uplifts with a late strong increase in the geotherm have also been observed in other parts of the European Variscides, usually associated with dome structures, as for example in NW-Spain (MARTINEZ et al., 1988).

The D_4-setting correlates broadly with the interval between the amphibole and biotite cooling ages in units III and IV, i.e. between 328 and 340 Ma. The minimum age of D_4 is given by the K/Ar biotite cooling age of a lamprophyric dike cross-cutting D_4-structures (HESS & SCHMIDT, 1989). At the end of D_4, all units were situated at roughly the same shallow level, crossing the 300°–isotherm between 330 and 320 Ma (KREUZER & HARRE, 1975; LIPPOLT, 1976). Extension continued into the Permian (MARELL, 1989) and denudation was terminated at the beginning of the Zechstein transgression.

8. Regional implications

The reconstruction of the crustal dynamics in the Odenwald allows an insight into the evolution of a magmatic arc developed at a transcurrent collision zone. Important clues can be given now to revise the geodynamic model for the Northern Mid-European Variszides:

Subsidence and sedimentation onto unit I and its prolongation to the SW occurred contemporaneously with sinistral D_3-strike slip movements which in turn were contemporaneous with subduction of oceanic crust under the Mid-German Crystalline Rise, as shown by voluminous calcalkaline intrusions. Strike slip movements at that time may have been initiated by oblique subduction and/or continental escape tectonics. Unit II, the area with the strongest strike slip movements is the area with the most voluminous and complete calcalkaline intrusion suite. Subsidence and sedimentation onto unit I may be interpreted as the consequence of crustal thinning, either due to horizontal extension normal to the D_3-sinistral shear zones (transtension; KROHE, 1991b), or to a major pull-apart basin confined by D_3 sinistral shear zones (Fig. 4).

Modern analogues to the Odenwald scenario (see Fig. 4 III) can be found in the area of the Burma/Sumatra active continental margin. Along this margin, oblique subduction of the Indian plate and lateral escape of continental fragments caused a complicated kinematic pattern, involving strike slip zones and the formation of pull-apart structures in the overriding plate (TAPPONNIER et al., 1986).

It is important to note that the Variscan deformational history recorded in the Odenwald is not compatible with that of the Rhenohercynian foreland. While crustal stacking occurred in the Rhenohercynian from 320–300 Ma (WEBER & BEHR, 1983; AHRENDT et al., 1983), uplift was almost terminated in the Odenwald. From the compilation of structural, geochronological and PT-data, it can be shown that in the Odenwald compressive tectonics did not occur later than 380–360 Ma. Afterwards, the D_3- and D_4-deformational events generally contain a component of horizontal extension effectively controlling the uplift. The Odenwald remained in an extensional setting until the Mid-Permian.

During the D_3- and D_4-events, the maximum horizontal stress was orientated roughly N-S. From D_3 to D_4, the vertical stress became the main stress component, but the orientation of the principal stresses remained constant (KROHE, 1991a). In the Rhenohercynian foreland, however, the maximum horizontal stress was roughly oriented NW-SE. This indicates that the Mid-German Crystalline Rise moved adjacent to the Rhenohercynian after the D_4-event. This final juxtaposition of both terranes may be due to late dextral strike slip movements as observed for instance by ONCKEN (1988) in the Northern Phyllite Zone and the southern Rhenohercynian.

Acknowledgements

We thank H.-D. Trochim for five samples from the collection of the Institut für Mineralogie Bochum and W. V. Maresch (Münster) as well as two anonymous reviewers for helpful critics.

References

AHRENDT, H., CLAUER, N., HUNZIKER, J.C. & WEBER, K. (1983): Migration of folding and metamorphism in the Rheinische Schiefergebirge deducted from K-Ar and Rb-Sr age determinations. – In: Martin, H. & Eder, F. W. (eds.): Intracontinental fold belts. – 323–338, Berlin (Springer).

ANDERSEN, D. J. & LINDSLEY, D. H. (1985): New (and final) models for the Ti-magnetite/ilmenite geothermometer and oxygen barometer. – EOS Transactions, **66,** 18, 416.

BERMAN, R. G. (1988): Internally-consistent thermodynamic data for minerals in the system Na_2O-K_2O-CaO-MgO-FeO-Fe_2O_3-Al_2O_3-SiO_2-TiO_2-H_2O-CO_2. – J. Petrol., **29,** 445–522.

– & BROWN, T. H. (1985): Heat capacity of minerals in the system Na_2O-K_2O-CaO-MgO-FeO-Fe_2O_3-Al_2O_3-SiO_2-TiO_2-H_2O-CO_2: representation, estimation, and high temperature extrapolation. – Contrib. Mineral. Petrol., **89,** 168–183.

BURNHAM, C. W. (1979): Magmas and hydrothermal fluids. – In: Barnes, H. L. (ed.): Geochemistry of hydrothermal ore deposits. – 71–136, New York (Wiley & Sons).

BÜSCH, W., MATTHES, S. & SCHUBERT, W. (1980): Zur genetischen Deutung der Kinzigite im Schwarzwald und Odenwald. – N. Jb. Mineral. Abh., **137,** 223–256.

CHATTERJEE, N. D. (1960): Geologische Untersuchungen im Kristallin des Böllsteiner Odenwaldes. – N. Jb. Geol. Paläont. Abh., **111,** 137–180.

– & JOHANNES, W. (1974): Thermal stability and standard thermodynamic properties of synthetic $2M_1$-muscovite, $KAl_2(AlSi_3O_{10}(OH)_2)$. – Contrib. Mineral. Petrol., **48,** 89–114.

DEKORP RESEARCH GROUP (1985): First results and preliminary

interpretation of deep reflection seismic recordings along the profile DEKORP 2S. – J. Geophys., **57,** 137–163.

FERRY, J. M. & SPEAR, F. S. (1978): Experimental calibration of the partitioning of Fe and Mg between biotite and garnet. – Contrib. Mineral. Petrol., **66,** 113–117.

FRANKE, W. (1989): Tectonostratigraphic units in the Variscan belt of central Europe. – Geol. Soc. Amer. Spec. Paper, **230,** 67–90.

HAMMARSTROM, J. M. & ZEN, E-AN. (1986): Aluminium in hornblende: an empirical igneous geobarometer. – American Mineralogist, **71,** 1297–1313.

HELLMANN, K.-N. (1975): Die Granodioritporphyrite des Bergsträßer Odenwaldes. – Aufschluß, **27,** 189–196.

–, LIPPOLT, H. J. & TODT, W. (1982): Interpretation der Kalium-Argon-Alter eines Odenwälder Granodioritporphyritganges und seiner Nebengesteine. – Aufschluß, **33,** 155–164.

HENES-KLAIBER, U., HOLL, A. & ALTHERR, R. (1989): The Odenwald: More evidence for Hercynian arc magmatism. – Terra abstracts, **1,** 1, 281.

HERZBERG, C. T. (1978): Pyroxene geothermometry and geobarometry: experimental and thermodynamic evaluation of some subsolidus phase relations involving pyroxenes in the system CaO-MgO-Al_2O_3-SiO_2. – Geochim. Cosmochim. Acta, **42,** 945–957.

HESS, J. C. & SCHMIDT, G. (1989): Zur Altersstellung der Kataklasite im Bereich der Otzberg-Zone, Odenwald. – Geol. Jb. Hessen, **117,** 69–77.

HOLDAWAY, M. J. (1971): Stability of andalusite and the aluminium silicate phase diagram. – Amer. J. Sci., **271,** 97–131.

– & LEE, S. M. (1977): Fe-Mg cordierite stability in high-grade pelitic rocks based on experimental, theoretical and natural observations. – Contrib. Mineral. Petrol., **63,** 175–198.

HOLLAND, T. J. B. & POWELL, R. (1990): An enlarged and updated internally consistent thermodynamic dataset with uncertainties and correlations: The system K_2O-Na_2O-CaO-MgO-MnO-FeO-Fe_2O_3-Al_2O_3-TiO_2-SiO_2-C-H_2-O_2. – J. Metamorph. Geol. **8,** 89–124.

HOLLISTER, L. S., GRISSOM, G. C., PETERS, E. K., STOWELL, H. H. & SISSON, V. B. (1987): Confirmation of the empirical correlation of Al in hornblende with pressure of solidification of calc-alkaline plutons. – American Mineralogist, **72,** 231–239.

HUSTIAK, D. & KROHE, A. (1990): Microstructural evidence for polyphase deformation in high-grade rocks of the NW-Odenwald, FRG. – Terra abstr., **2,** 14.

JOHANNES, W. (1984): The significance of experimental studies for the formation of migmatites. – In: Ashworth, J. R. (ed.): Migmatites. – 36–85, Glasgow (Blackie).

KIRSCH, H. (1984): Die Alter einiger variszischer Plutonite und Vulkanite des Odenwaldes und des nördlichen Oberrheingrabens ($^{40}Ar/^{39}Ar$-Untersuchungen). – Unpubl. Diploma thesis Univ. Heidelberg, 122 p.

–, KOBER, B. & LIPPOLT, H. J. (1988): Age of intrusion and rapid cooling of the Frankenstein gabbro (Odenwald, SW-Germany) evidenced by $^{40}Ar/^{39}Ar$ and single-zircon $^{207}Pb/^{206}Pb$ measurements. – Geol. Rundschau, **77,** 3, 639–711.

KREUZER, H. & HARRE, W. (1975): K/Ar-Altersbestimmungen an Hornblenden und Biotiten des Kristallinen Odenwaldes. – Aufschluß, **27,** 71–77.

KROHE, A. (1991a): Amalgamation, uplift and exhumation of intermediate crustal rocks in the Variscan Odenwald (SW-Germany) – Tectonic setting and deformation mechanism path. – Tectonophysics (in press).

– (1991b): Emplacement of synkinematic plutons in the Variscan Odenwald (Germany) controlled by transtensional tectonics. – Geol. Rundschau (this volume).

KNAUER, E., OKRUSCH, M., RICHTER, P., SCHMIDT, K. & SCHUBERT, W. (1974): Die metamorphe Basit-Ultrabasit-Assoziation in der Böllsteiner Gneiskuppel, Odenwald. – N. Jb. Mineral. Abh., **122,** 186–228.

LENZ, H. & MÜLLER, P. (1976): Radiometrische Altersbestimmung am Kristallin der Bohrung Saar 1. – Geol. Jb., **A27,** 429–432.

LIEW, T. C. & HOFMANN, A.W. (1988): Precambrian crustal components, plutonic associations, plate environment of the Hercynian Fold Belt of Central Europe: Indications from a Nd and Sr isotopic study. – Contrib. Mineral. Petrol., **98,** 129–138.

LINDSLEY, D. H. (1983): Pyroxene thermometry. – American Mineralogist, **68,** 477–493.

LIPPOLT, H. J. (1986): Nachweis altpaläozoischer Primäralter (Rb-Sr) und karbonischer Abkühlungsalter (K-Ar) der Muskowit-Biotit-Gneise des Spessarts und der Biotitgneise des Böllsteiner Odenwaldes. – Geol. Rundschau, **75,** 3, 569–583.

LORENZ, V. & NICHOLLS, I. A. (1984): Plate and intraplate processes of Hercynian Europe during the Late Paleozoic. – Tectonophysics, **107,** 25–56.

MAGGETTI, M. (1975): Die Tiefengesteine des Bergsträßer Odenwaldes. – Aufschluß, **27,** 87–107.

MARELL, D. (1989): Das Rotliegende zwischen Odenwald und Taunus. – Geol. Abh. Hessen, **89,** 128 p.

MARTINEZ, F. J., JULIVERT, M., SEBASTIAN, A., ARBOLEYA, M. L. & GIL IBARGUCHI, J. I. (1988): Structural and thermal evolution of high-grade areas in the northwestern parts of the Iberian Massif. – Am. J. Sci., **288,** 969–996.

MASSONNE, H.-J. (1984): Bestimmung von Intrusionstiefen variszischer Granite Mitteleuropas und Neuschottlands anhand der Chemie ihrer Hellglimmer. – Fortschr. Mineral., **62,** Beiheft 1, 147–148.

– (1988): New experimental results in the system K_2O-MgO-Al_2O_3-SiO_2-H_2O (KMASH) on medium- and high-grade metamorphism of pelitic rocks. – Terra cognita, **8,** 1, 71.

–, – (1983): A new experimental phengite barometer and its application to a Variscan subduction zone at the southern margin of the Rhenohercynicum. – Terra Cognita, **3,** 187.

– & SCHREYER, W. (1987): Phengite geobarometry based on the limiting assemblage with K-feldspar, phlogopite and quartz. – Contrib. Mineral. Petrol., **96,** 212–224.

MATTHES, S. & SCHUBERT, W. (1971): Der Original-Beerbachit im Odenwald, ein Amphibolit-Hornfels in Pyroxen-Hornfelsfazies. – Contr. Mineral. Petrol., **33,** 62–86.

NEUGEBAUER, J. (1988): The Variscan plate tectonic evolution: an improved «Iapetus model«. – Schweiz. Mineral. Petrogr. Mitt., **68,** 313–333.

NICKEL, E. (1985): Odenwald. – Sammlung Geologischer Führer, **65,** 231 pp., Berlin (Bornträger).

– & MAGGETTI, M. (1974): Magmenentwicklung und Dioritbildung im synorogen konsolidierten Grundgebirge des Bergsträßer Odenwaldes. – Geol. Rundschau, **63,** 618–654.

OKRUSCH, M. (1983): The Spessart crystalline complex, NW Bavaria. – Fortschr. Mineral., **62,** Beiheft 2, 135–169.

–, VON RAUMER, J., MATTHES, S. & SCHUBERT, W. (1975): Mineralfazies und Stellung der Metamorphite im kristallinen Odenwald. – Aufschluß, **27,** 109–134.

ONCKEN, O. (1988): Geometrie und Kinematik der Taunuskammüberschiebung – Beitrag zur Diskussion des Dekkenproblems im südlichen Schiefergebirge. – Geol. Rundschau, **77,** 551–575.

Pflug, H. D. & Reitz, E. (1987): Palynology in metamorphic rocks; indication of early land plants. – Naturwissenschaften, **74,** 386–387.

Plyusnina, L. P. (1982): Geothermometry and geobarometry of plagioclase-hornblende bearing assemblages. – Contrib. Mineral. Petrol., **80,** 140–146.

Raase, P. (1974): Al and Ti contents of hornblende, indicators of pressure and temperature of regional metamorphism. – Contrib. Mineral. Petrol., **45,** 231–236.

Rittmann, K. L. (1984): Argon in Hornblende, Biotit und Muskovit bei der geologischen Abkühlung – $^{40}Ar/^{39}Ar$-Untersuchungen. – Unpubl. PhD thesis Univ. Heidelberg, 278 p.

Spear, F. S. (1980): NaSi — CaAl exchange equilibrium between plagioclase and amphibole. – Contrib. Mineral. Petrol., **72,** 33–41.

— & Selverstone, J. (1983): Quantitative P-T paths from zoned minerals: theory and tectonic applications. – Contrib. Mineral. Petrol., **83,** 348–357.

Spencer, K. J. & Lindsley, D. H. (1981): A solution model for coexisting iron-titanium oxides. – American Mineralogist, **66,** 1189–1201.

Tapponnier, P., Peltzer, G. & Armijo, R. (1986): On the mechanics of the collision between India and Asia. – In: Coward, M. P. & Ries, A. C. (eds.): Collision tectonics. – Geol. Soc. London Spec. Pub., **19,** 115–158, London (Blackwell).

Todt, W. (1979): U-Pb-Datierungen an Zirkonen des kristallinen Odenwaldes. – Fortschr. Miner., **57,** Beiheft 1, 153–154.

Trochim, H. D. (1960): Zur Petrogenese des Gabbro-Plutons vom Frankenstein (Odenwald). – Unpubl. PhD thesis Univ. Freiburg, 150 p.

Von Raumer, J. F. (1973): Die mineralfazielle Stellung der Metapelite und Metagrauwacken zwischen Heppenheim und Reichelsheim (Odenwald). – N. Jb. Mineral. Abh., **118,** 313–336.

Weber, K. & Behr, H. J. (1983): Geodynamic interpretation of the Mid-European Variscides. – In: Martin, H. & Eder, F. W. (eds.): Intracontinental fold belts. – 427–469, Berlin (Springer).

Wells, P. R. A. (1977): Pyroxene thermometry in simple and complex systems. – Contr. Mineral. Petrol., **62,** 129–139.

Zen, E-An. (1989): Wet and dry AFM mineral assemblages of strongly peraluminous granites. – EOS Transactions, **70,** 109–110.

Zimmerle, W., Hering, O., Ghazanfari, A., Krebs, W. & Weber, G. (1976): Die Tiefbohrung Saar 1 – Petrographische Beschreibung und Deutung der erbohrten Schichten. – Geol. Jb., **A27,** 91–305.